Penerbit Akademia Baru

Journal of Advanced Research in Fluid Mechanics and Thermal Sciences

Journal homepage: www.akademiabaru.com/arfmts.html
ISSN: 2289-7879

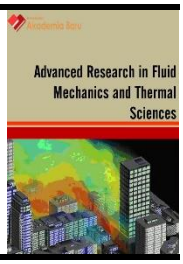

MHD Viscous Incompressible Casson Fluid Flow with Hall Current

Open Access

Mohammad Afikuzzaman[1], Mohammad Ferdows[2,*], Raushan Ara Quadir[3], Md. Mahmud Alam[1]

[1] Mathematics Discipline, Khulna University, Khulna-9208, Bangladesh
[2] Research group of Fluid Flow Modeling and Simulation, Department of Applied Mathematics, University of Dhaka, Dhaka-1000, Bangladesh
[3] School of Mathematics, Statistics and Computer Science, University of KawaZulu-Natal, South Africa

ARTICLE INFO

Article history:
Received 30 March 2019
Received in revised form 27 May 2019
Accepted 16 July 2019
Available online 30 August 2019

Keywords:
MHD flow; Free convection; EFDM; Stability analysis and Hall current

ABSTRACT

An electrically conducting free convection and mass transfer viscous incompressible Casson fluid bounded by two parallel non-conducting plates have been investigated in the presence of hall current for two dimensional case. Initially the fluid motion is constant at the upper plate and the uniform magnetic field is applied perpendicular to the plate. The lower plate is stationary and the upper plate is moving. Explicit finite difference method (EFDM) has been used to solve the partial coupled non-linear momentum, energy and concentration equations. The stability conditions and convergence criteria of the finite difference scheme are established for finding the restriction of the values of various parameters to get converse solution. The influence of various interesting parameters on the flow has been analysed and discussed through graph in details. The values of Shear Stress, Nusselt number and Sherwood number for both moving and stationary plates for different physical parameters have been investigated in the form of graphical representation. For all cases, it is accomplished that, shear stress, Nusselt number and Sherwood numbers are increased with the increase of Soret number(S_r).

Copyright © 2019 PENERBIT AKADEMIA BARU - All rights reserved

1. Introduction

The fluid flow between parallel plates by means of Couetee motion is a classical fluid mechanics problem that has applications in magneto hydrodynamic (MHD), power generators, MHD pumps, aerodynamics heating, polymer extrusion, petroleum industry, pharmaceutical process, purification of crude oil, fluid droplet sprays, metal forming, wire and glass fibre drawing and several others. The industrial applications of non-Newtonian Casson fluid flow are increasing day by day. Some fluids behave like elastic solids, and for those fluids, a yield shear stress exists in the constitutive equations. Casson fluid is one of such non-Newtonian fluids. If the shear stress magnitude is greater than the yield shear stress, then flow occurs. The non-linear Casson's constitutive equation has been found to describe accurately the flow curves of suspensions of pigments in lithographic varnishes used for

* *Corresponding author.*
E-mail address: ferdows@du.ac.bd (Mohammad Ferdows)

preparation of printing inks and silicon suspensions. Jha and Apere [1] studied the Magneto hydrodynamic effect on the formation of Couette flow. Soundalgekar *et al*., [2] considered Hall and Ion-slip effects in MHD Couette flow with heat transfer in the same problem. Das and Batra [3] investigated Secondary flow of a Casson fluid in a slightly curved tube. Attia and Kotb [4] discussed MHD flow between two parallel plates with hall current. Many authors [5-10] investigated the flow and heat transfer of a non-Newtonian flow. Attia and Ahmed [11] analysed Hydrodynamic impulsive Lid driven flow and heat transfer of a Casson fluid. Sayed-Ahmed *et al*., [12] investigated time dependent pressure gradient effect on unsteady MHD Couetee flow and heat transfer of a Casson fluid. Afikuzzaman *et al*., [13-15] extended the work of Sayed-Ahmed *et al*., [9]'s model from different aspects and used explicit finite difference method (EFDM). In very recent times, different authors have investigated Casson fluid from different perspective [16-20].

Hence our main aim is to extend the work [14] in the case of two dimension problem and to investigate MHD viscous incompressible Casson fluid flow with hall current for different interesting parameters such as Magnetic parameters (M), Permeability of porous medium (γ), Eckert number (E_c), Prandtl number (P_r), Schmidt number (S_c), Soret number (S_r), Grashoff number (G_r), Modified Grashoff number (G_m). The proposed model has been transformed into nonlinear coupled partial differential equations by usual transformation. Finally, the comparison of the current results with the previous [14] has been presented.

2. Mathematical Formulations

The fluid is assumed viscous, laminar and incompressible flows between two infinite horizontal plates located at $y=\pm h$ planes and extended from $x=-\infty$ to ∞ and from $z=-\infty$ to ∞. The lower plate is stationary while the upper plate moves with a constant velocity U_o (Figure 1).

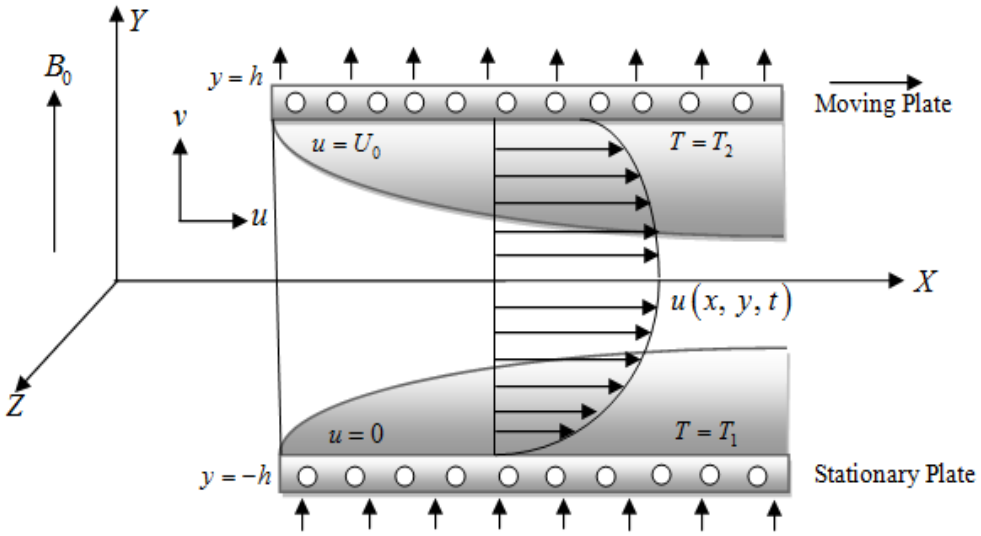

Fig. 1. Geometrical configuration of boundary layer

The upper and lower plates are kept at two constants temperature respectively T_2 and T_1 with $T_2>T_1$ and concentration c_2 and c_1 with $c_2>c_1$. The fluid is acted upon by a constant pressure gradient, a uniform suction from above and injection from below which are applied at $t=0$. A uniform magnetic field is applied in the positive *y*-direction and is assumed undistributed as the induced magnetic field is neglected by assuming a very small magnetic Reynolds number. The Hall Effect is taken into consideration and consequently a z-component for the velocity is expected to arise. The

uniform suction implies that the *y*-component of the velocity v_0 is constant. Thus, the fluid velocity vector is given by

$$v = u\mathbf{i} + v_O\mathbf{j} + w\mathbf{k} \tag{1}$$

By using generalized Ohm's law, the MHD free convection and mass transfer fluid flows are governed by the following equations.

Continuity equation

$$\frac{\partial u}{\partial x} + \frac{\partial v}{\partial y} = 0 \tag{2}$$

Momentum equation in *x* and *z* direction

$$\frac{\partial u}{\partial t} + u\frac{\partial u}{\partial x} + v\frac{\partial u}{\partial y} = -\frac{1}{\rho}\frac{\partial p}{\partial x} + g\beta(T - T_1) + g\beta^*(C - C_1) + \frac{1}{\rho}\left[\frac{\partial}{\partial y}\left(\mu\frac{\partial u}{\partial y}\right)\right]$$
$$-\frac{\nu}{k}u - -\frac{1}{\rho}\left[\frac{\sigma B_o^{\,2}}{1+m^2}(u + mw)\right] \tag{3}$$

$$\frac{\partial w}{\partial t} + u\frac{\partial w}{\partial x} + v\frac{\partial w}{\partial y} = \frac{1}{\rho}\left[\frac{\partial}{\partial y}\left(\mu\frac{\partial w}{\partial y}\right)\right] - \frac{\nu}{k}w - \frac{1}{\rho}\frac{\sigma B_o^{\,2}}{1+m^2}(w - mu) \tag{4}$$

Energy equation

$$\frac{\partial T}{\partial t} + u\frac{\partial T}{\partial x} + v\frac{\partial T}{\partial y} = \frac{k}{\rho c_p}\frac{\partial^2 T}{\partial y^2} + \frac{\mu}{\rho c_p}\left[\left(\frac{\partial u}{\partial y}\right)^2 + \left(\frac{\partial w}{\partial y}\right)^2\right] + \frac{1}{\rho c_p \sigma}\frac{\sigma B_o^{\,2}}{1+m^2}\left(u^2 + w^2\right) \tag{5}$$

The corresponding boundary conditions are

$t \geq 0 \quad u = 0,\ w = 0,\ T = T_1,\ C = C_1$ at $y = -h$

$u = U_o,\ w = 0,\ T = T_2,\ C = C_2$ at $y = h$

The non-dimensional variables that have been used in the governing equations are

$$\bar{x} = \frac{xU_o}{\nu},\ \bar{y} = \frac{yU_o}{\nu},\ \bar{t} = \frac{tU_o^2}{\nu},\ \bar{u} = \frac{u}{U_o},\ \bar{w} = \frac{w}{U_o},\ \bar{v} = \frac{v}{U_o},\ \bar{p} = \frac{p}{\rho U_o^2},\ \bar{C} = \frac{C - C_1}{C_2 - C_1},$$
$$\theta = \frac{T - T_1}{T_2 - T_1},\ \bar{\mu} = \frac{\mu}{K_c{}^2}$$

Using these above dimensionless variables, the following dimensionless equations have been as

$$\frac{\partial u}{\partial t}+u\frac{\partial u}{\partial x}+v\frac{\partial u}{\partial y}=-\alpha e-dt+\frac{\partial^2 u}{\partial y^2}+G_r\theta+G_m C-\gamma u-\frac{M}{1+m^2}(u+mw) \tag{7}$$

$$\frac{\partial w}{\partial t}+u\frac{\partial w}{\partial x}+v\frac{\partial w}{\partial y}=\frac{\partial^2 w}{\partial y^2}-\gamma w-\frac{M}{1+m^2}(w-mu) \tag{8}$$

$$\frac{\partial \theta}{\partial t}+u\frac{\partial \theta}{\partial x}+v\frac{\partial \theta}{\partial y}=\frac{1}{P_r}\frac{\partial^2 \theta}{\partial y^2}+\frac{E_c M}{1+m^2}(u^2+w^2)+E_c\left[\left(\frac{\partial u}{\partial y}\right)^2+\left(\frac{\partial w}{\partial y}\right)^2\right] \tag{9}$$

$$\frac{\partial C}{\partial t}+u\frac{\partial C}{\partial x}+v\frac{\partial C}{\partial y}=\frac{1}{S_c}\frac{\partial^2 C}{\partial y^2}+S_r\frac{\partial^2 \theta}{\partial y^2} \tag{10}$$

The corresponding non-dimensional boundary conditions are

$t>0,\quad u=0,\quad w=0,\quad \theta=0,\quad C=0$ for $y=-1$

$u=1,\quad w=0,\quad \theta=1,\quad C=1$ for $y=1$

The non-dimensional quantities are: Magnetic parameter $M=\frac{\sigma B_o{}^2 \nu}{\rho U_O{}^2}$, Permeability of the porous medium $\gamma=\frac{\nu^2}{kU_O{}^2}$, Eckert number $E_c=\frac{U_O{}^2}{C_p(T_2-T_1)}$, Prandtl number $P_r=\frac{\rho C_p \nu}{k}$, Schmidt number $S_c=\frac{\nu}{D_m}$, Soret number $S_r=\frac{D_m K_t(T_2-T_1)}{\nu T_m(C_2-C_1)}$, Grashoff number $G_r=\frac{g\beta(T_2-T_1)\nu}{U_o^3}$, Modified Grashoff number $G_m=\frac{g\beta^*(C_2-C_1)\nu}{U_o^3}$.

2.1 Shear Stress, Nusselt and Sherwood Number

From the velocity field, the effects of various parameters on Shear Stress have been studied. The dimensionless Shear stress for moving and stationary wall respectively is given by;

$$\tau_{w1}=\left[\left[\left(\left(\frac{\partial u}{\partial y}\right)^2+\left(\frac{\partial w}{\partial y}\right)^2\right)^{\frac{1}{4}}+\frac{\tau_D^{1/2}}{\left(\left(\frac{\partial u}{\partial y}\right)^2+\left(\frac{\partial w}{\partial y}\right)^2\right)^{\frac{1}{4}}}\right]^2\right]_{y=-1}, \tau_{w2}=\left[\left[\left(\left(\frac{\partial u}{\partial y}\right)^2+\left(\frac{\partial w}{\partial y}\right)^2\right)^{\frac{1}{4}}+\frac{\tau_D^{1/2}}{\left(\left(\frac{\partial u}{\partial y}\right)^2+\left(\frac{\partial w}{\partial y}\right)^2\right)^{\frac{1}{4}}}\right]^2\right]_{y=1}$$

The dimensionless Nusselt number and Sherwood number at the moving wall and stationary wall is respectively given by;

$$Nu_1=\frac{\left(2\frac{\partial T}{\partial y}\right)_{y=1}}{T_m-1}, Nu_2=\frac{\left(2\frac{\partial T}{\partial y}\right)_{y=-1}}{-T_m}, \text{ and } Cu_1=\frac{\left(2\frac{\partial C}{\partial y}\right)_{y=1}}{C_m-1}, Cu_2=\frac{\left(2\frac{\partial C}{\partial y}\right)_{y=-1}}{-C_m}$$

where, T_m and C_m are the dimensionless mean value temperature and dimensionless mean value concentration respectively.

3. Numerical Solution

To obtain the difference equations the region of the flow is divided into a grid of lines parallel to X and Y axis where X -axis is taken along the plate and Y -axis is normal to the plate. It is considered that the plate of height is $X_{max}(=100)$ i.e. X varies from 0 to 100 and regard $Y_{max}(=2)$ i.e. Y varies from -1 to 1. There are $m=140$ and $n=140$ grid spacing in the X and Y directions respectively as shown in Figure 2. Hence the constant mesh size along X and Y directions respectively.

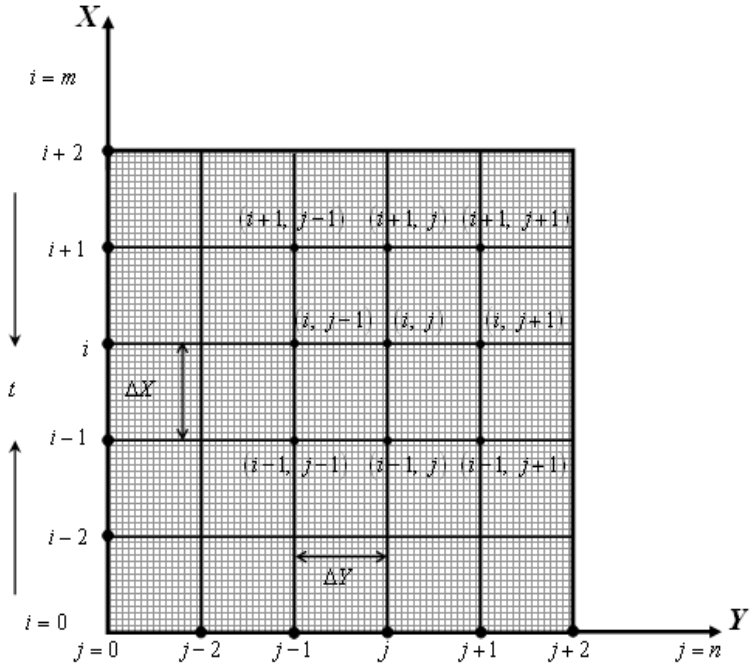

Fig. 2. Two dimensional finite difference grid spaces

$\Delta X = 0.71429 (0 \le X \le 100), \Delta Y = 0.01429 (-1 \le y \le 1)$ with smaller time step $\Delta t = 0.0001$.

Let $U^{n+1}, W^{n+1}, \theta^{n+1}$ *and* C^{n+1} denote the values U^n, W^n, θ^n *and* C^n at the end of a time step respectively. The explicit finite difference approximation gives;

$$\frac{U_{i,j}^{n+1} - U_{i,j}^n}{\Delta t} + U_{i,j}^n \frac{U_{i,j}^n - U_{i-1,j}^n}{\Delta X} + + V_{i,j}^n \frac{U_{i,j+1}^n - U_{i,j}^n}{\Delta Y} = -\alpha e^{-dt} + G_r \theta_{i,j}^n + G_m C_{i,j}^n$$
$$+ \frac{U_{i,j+1}^n - 2U_{i,j}^n + U_{i,j-1}^n}{\Delta Y^2} - \gamma U_{i,j}^n - \frac{M}{1+m^2}\left(U_{i,j}^n + m W_{i,j}^n\right) \quad (11)$$

$$\frac{W_{i,j}^{n+1} - W_{i,j}^n}{\Delta t} + U_{i,j}^n \frac{W_{i,j}^n - W_{i-1,j}^n}{\Delta X} + + V_{i,j}^n \frac{W_{i,j+1}^n - W_{i,j}^n}{\Delta Y} = \frac{W_{i,j+1}^n - 2W_{i,j}^n + W_{i,j-1}^n}{\Delta Y^2} - \gamma W_{i,j}^n$$
$$- \frac{M}{1+m^2}\left(W_{i,j}^n - m U_{i,j}^n\right) \quad (12)$$

$$\frac{\theta_{i,j}^{n+1} - \theta_{i,j}^n}{\Delta t} + U_{i,j}^n \frac{\theta_{i,j}^n - \theta_{i-1,j}^n}{\Delta X} + + V_{i,j}^n \frac{\theta_{i,j+1}^n - \theta_{i,j}^n}{\Delta Y} = \frac{1}{P_r}\left[\frac{\theta_{i,j+1}^n - 2\theta_{i,j}^n + \theta_{i,j-1}^n}{\Delta Y^2}\right]$$
$$+ E_c\left[\left(\frac{U_{i,j+1}^n - U_{i,j}^n}{\Delta Y}\right)^2 + \left(\frac{W_{i,j+1}^n - W_{i,j}^n}{\Delta Y}\right)^2\right] + \frac{E_c M}{1+m^2}\left[\left(U_{i,j}^n\right)^2 + \left(W_{i,j}^n\right)^2\right] \quad (13)$$

$$\frac{C_{i,j}^{n+1} - C_{i,j}^n}{\Delta t} + U_{i,j}^n \frac{C_{i,j}^n - C_{i-1,j}^n}{\Delta X} + V_{i,j}^n \frac{C_{i,j+1}^n - C_{i,j}^n}{\Delta Y} = \frac{1}{S_c} \frac{C_{i,j+1}^n - 2C_{i,j}^n + C_{i,j-1}^n}{\Delta Y^2} + S_r \frac{\theta_{i,j+1}^n - 2\theta_{i,j}^n + \theta_{i,j-1}^n}{\Delta Y^2} \quad (14)$$

The boundary conditions with the finite difference scheme are

$t > 0,$ $U_{i,-1}^n = 0,$ $W_{i,-1}^n = 0,$ $\theta i_{i,-1}^n = 0,$ $C_{i,-1}^n = 0$ *where* $L = -1$

$U_{i,1}^n = 1,$ $W_{i,1}^n = 0,$ $\theta_{i,1}^n = 1,$ $C_{i,1}^n = 1$ *where* $L = 1$

Here the subscripts i and j designate the grid points with X and Y coordinates respectively and the superscript n represents a value of time, $t = n\Delta t$ where $n = 0,1,2\ldots\ldots$. The numerical values of the Shear stresses are evaluated by five point approximate formula. Also the numerical values of Nusselt number and Sherwood number are calculated by five point approximation and trapezoidal numerical integration rule. The stability conditions of the method are

$\frac{2\Delta t}{(\Delta Y)^2 P_r} + U\frac{\Delta T}{\Delta X} + \left|-V\right|\frac{\Delta t}{\Delta Y} \le 1, U\frac{\Delta t}{\Delta X} + \left|-V\right|\frac{\Delta t}{\Delta Y} + \frac{2\Delta t}{S_c(\Delta Y)^2} \le 1$ and the convergence criteria $P_r \ge 0.50$ $S_C \ge 0.50$ which are not shown for brevity.

4. Results and Discussion

To obtain the steady-state solutions, the computations have been carried out up to dimensionless time $t=0$ to 20. The results of the computations, however, show little changes in the above mentioned quantities after dimensionless time $t=5$. Thus, the solutions for dimensionless time $t=5$ are essentially steady-state solutions. To observe the physical situation of the problem, the steady-state solutions have been illustrated in Figure 3 to 6.

The influence of magnetic parameter, M on the primary velocity, the secondary velocity are presented in Figure 3 and 4 respectively. It is shown from Figure 3 and 4, the primary velocity U decreases where the secondary velocity W increases with the increase of M.

The effect of Magnetic parameter M on shear stress, temperature distributions and concentration distributions are presented in Figure 5 to 9 respectively. It is observed that shear stress decreases in Figure 5 and 6 with the increase of M. The temperature distributions θ are decreased while concentration distributions C found minor decreasing effects at the rise of M which are illustrated in Figure 7 and 8 respectively.

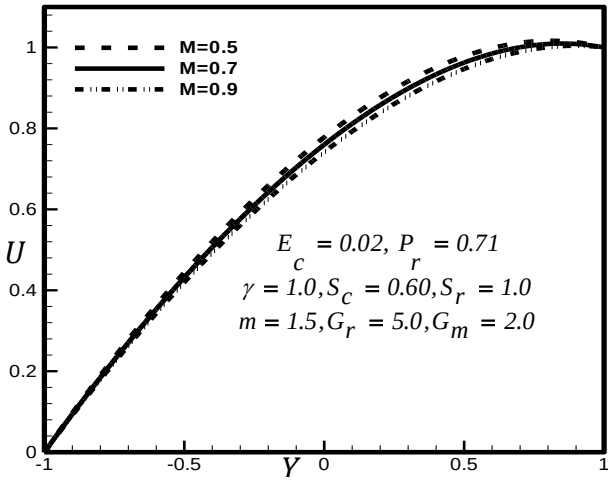

Fig. 3. Primary velocity versus Y at different values of Magnetic parameter at t=5.0

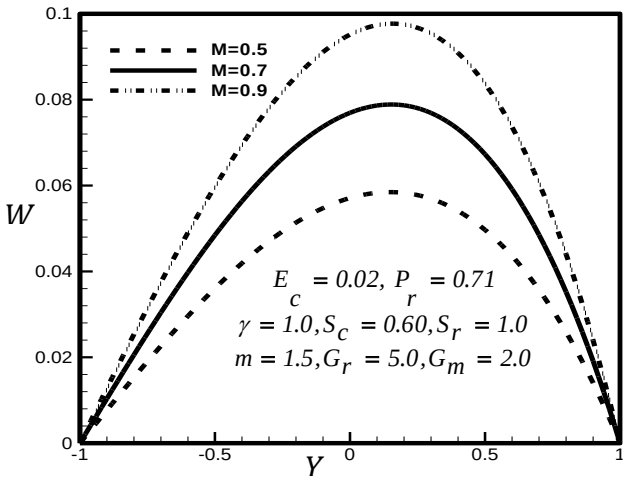

Fig. 4. Secondary velocity versus Y at different values of Magnetic parameter at t=5.0

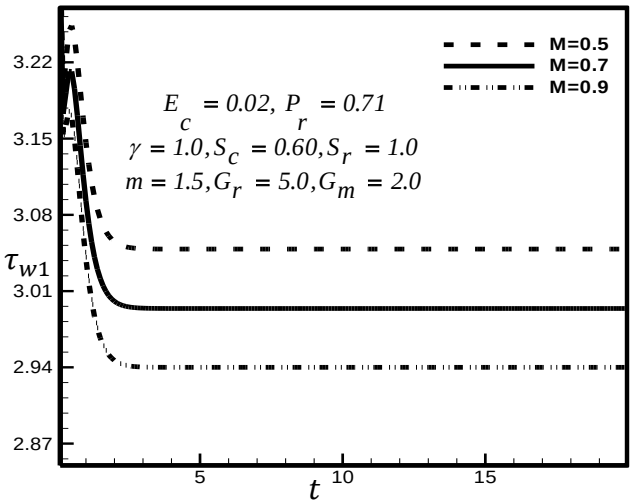

Fig. 5. Shear Stress at moving plate for different values of Magnetic parameter at $t=5.0$

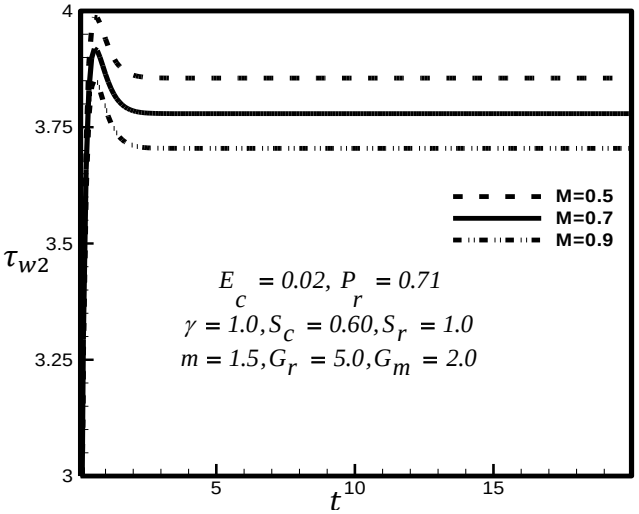

Fig. 6. Shear stress at stationary plate for different values of Magnetic parameter at $t=5.0$

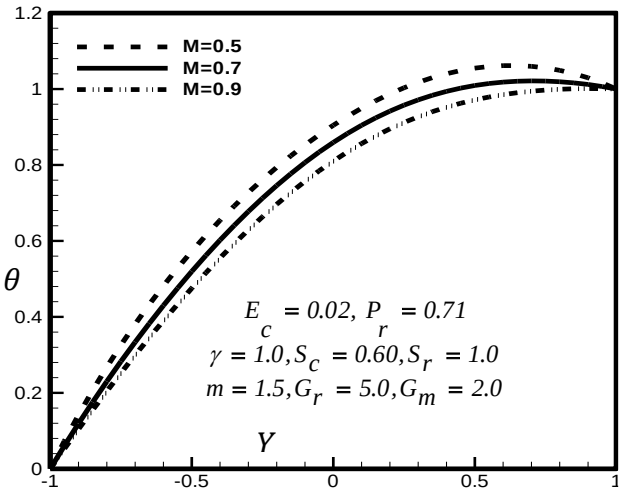

Fig. 7. Temperature versus Y at different values of Magnetic parameter at $t = 5.0$

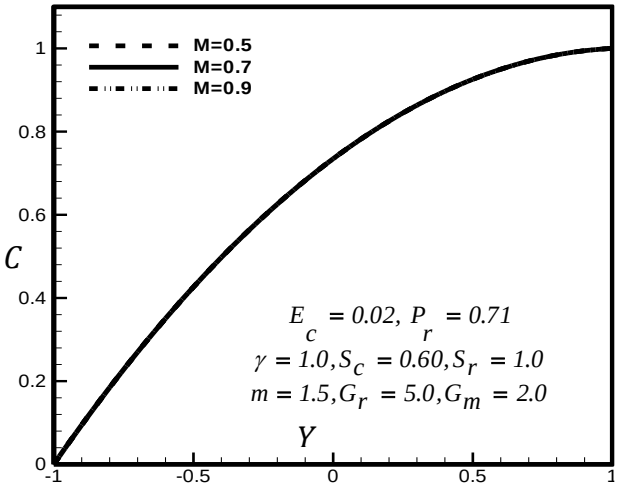

Fig. 8. Concentration versus Y at different values of Magnetic parameter at $t = 5.0$

The influence of Magnetic parameter M on nusselt number, and sherwood number are illustrated in Figure 9 to 12 respectively. It is observed that nusselt number and sherwood number profiles for both plates are decreased with the increase of M . Such type of behavior is occurred due to moving and stationary plates.

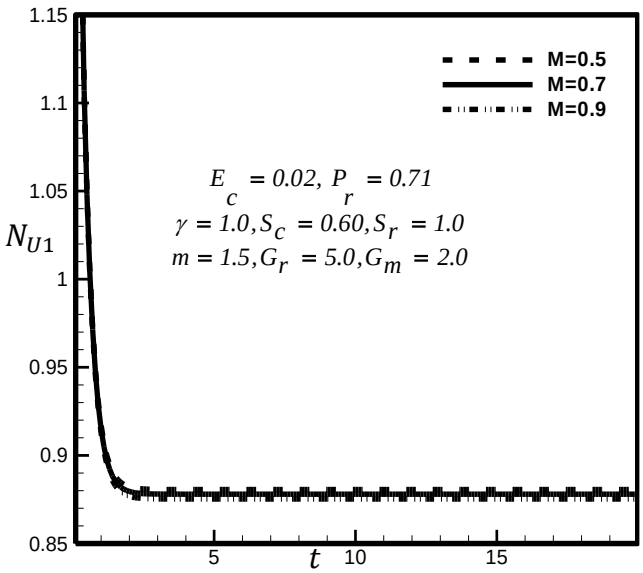

Fig. 9. Nusselt number at moving plate for different values of Magnetic parameter at $t = 5.0$

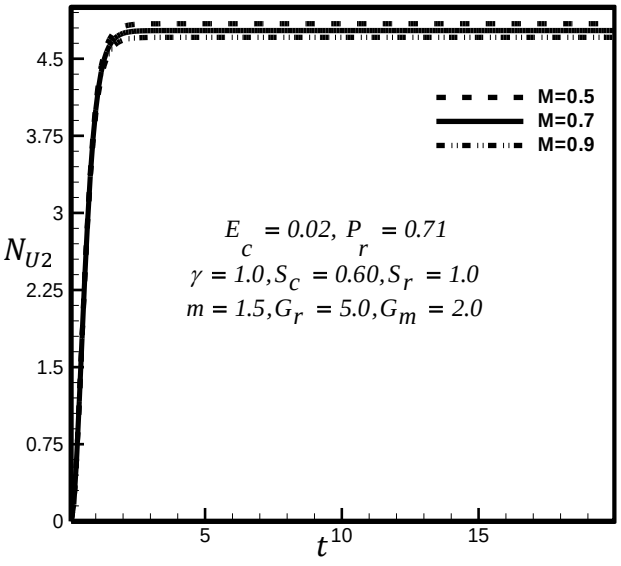

Fig. 10. Nusselt number at stationary plate for different values of Magnetic parameter at $t = 5.0$

The effect of Soret number S_r on primary velocity, secondary velocity and shear stress are presented in Figure 13 to 16 respectively. The primary velocity U and secondary velocity W are increased with the increase of S_r which are shown in Figure 13 and 14.

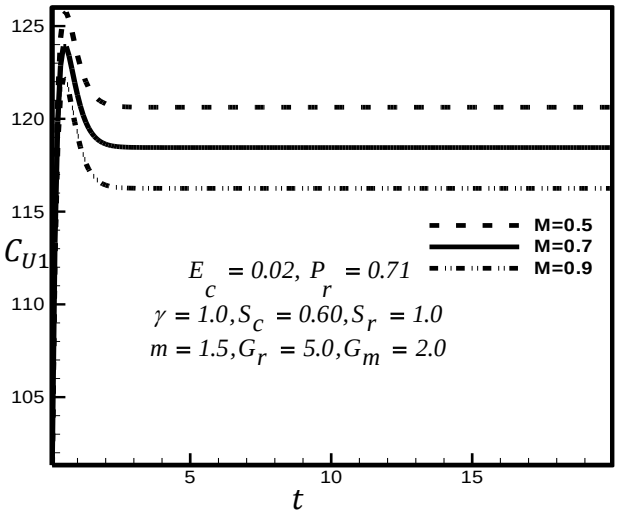

Fig. 11. Sherwood number at moving plate for different values of Magnetic parameter at $t = 5.0$

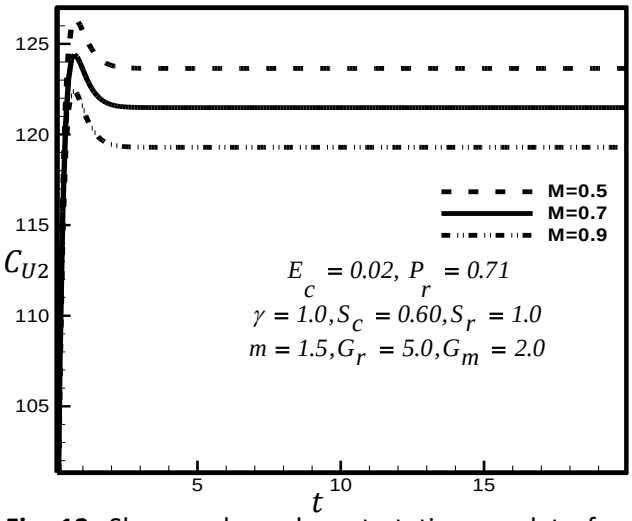

Fig. 12. Sherwood number at stationary plate for different values of Magnetic parameter at $t = 5.0$

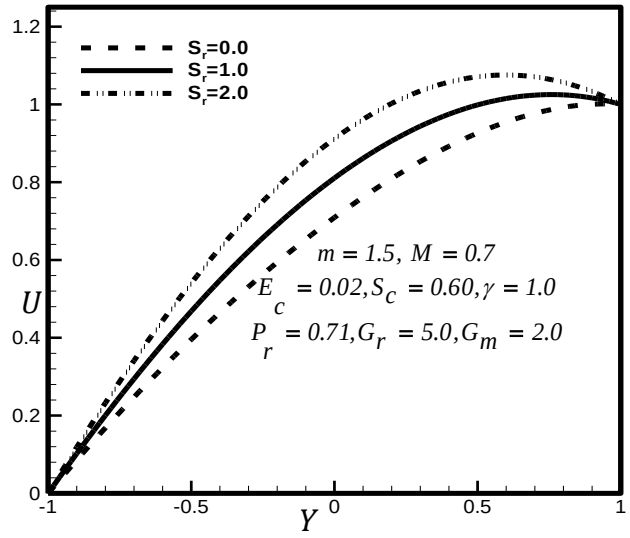

Fig. 13. Primary velocity versus Y at different values of Soret number at $t = 5.0$

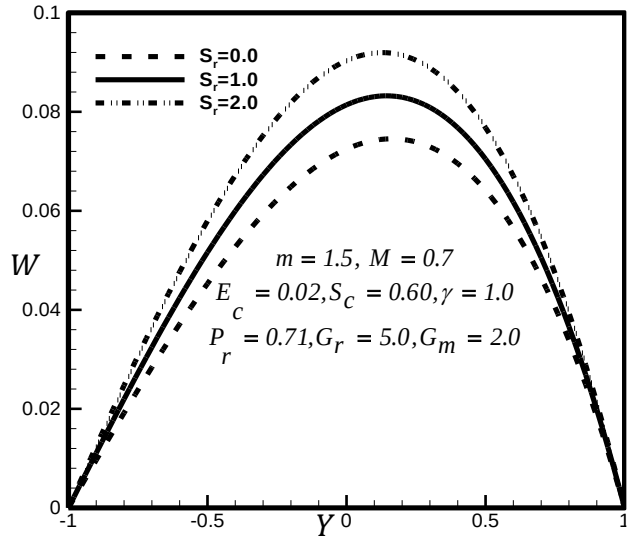

Fig. 14. Secondary velocity versus Y at different values of Soret number at $t = 5.0$

The shear stress profiles both in upper and lower plates are increased with the increase of S_r which are shown in Figure 15 and 16 respectively. The effect of Soret number S_r temperature distributions and concentration distributions are presented in Figure 17 and 18 respectively. Both the temperature and concentration distributions are increased with the increase of S_r. Such type behaviour is occurred due to thermal diffusion ratio.

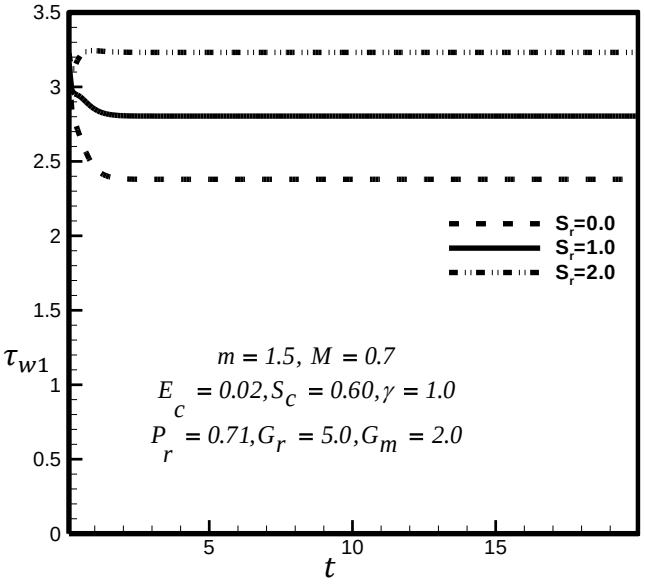

Fig. 15. Shear Stress at moving plate for different values of Soret number at $t = 5.0$

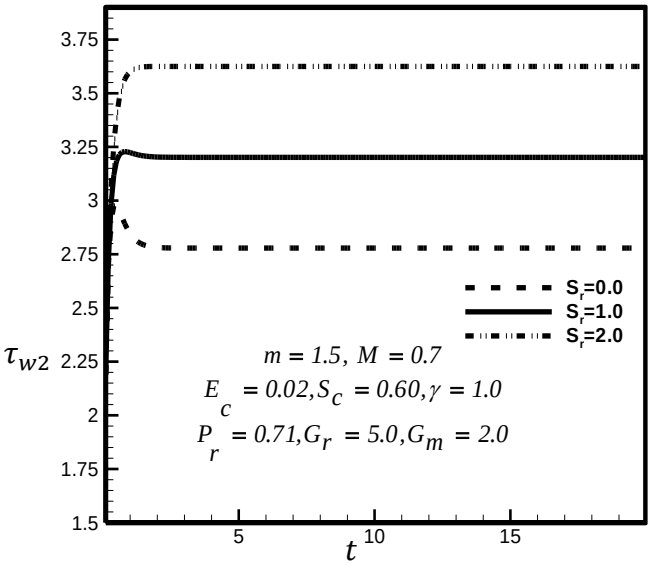

Fig. 16. Shear Stress at stationary plate for different values of Soret number at $t = 5.0$

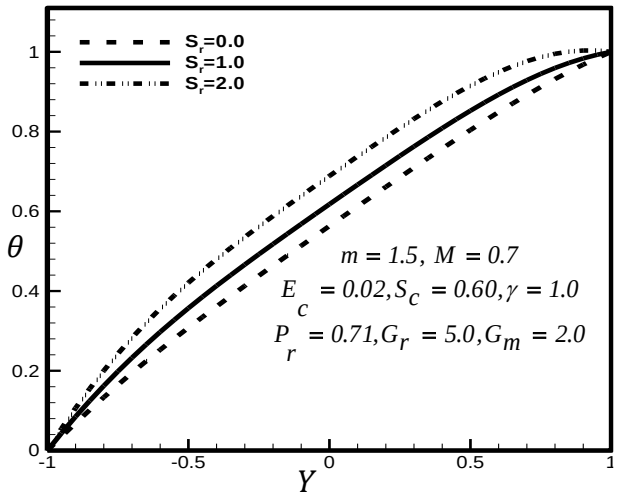

Fig. 17. Temperature versus Y at different values of Soret number at $t = 5.0$

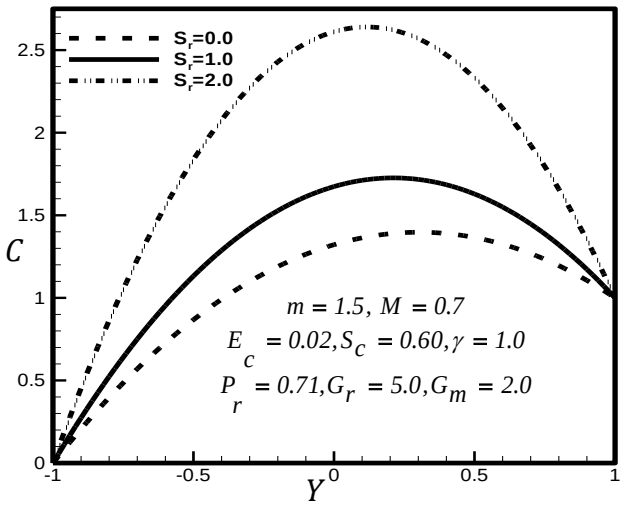

Fig. 18. Concentration versus Y at different values of Soret number at $t = 5.0$

The nusselt number and Sherwood number profiles both in upper and lower plates are increased with the increase of S_r which are shown in Figure 19 to 22 respectively. Such type behaviour is occurred due to thermal diffusion ratio.

Finally, a comparison of the present steady-state results with the published results of Afikuzzaman and Alam [14] has been discussed. The accuracy of the present results is qualitatively similar but quantitatively good in case of all the flow parameters (Figure 23).

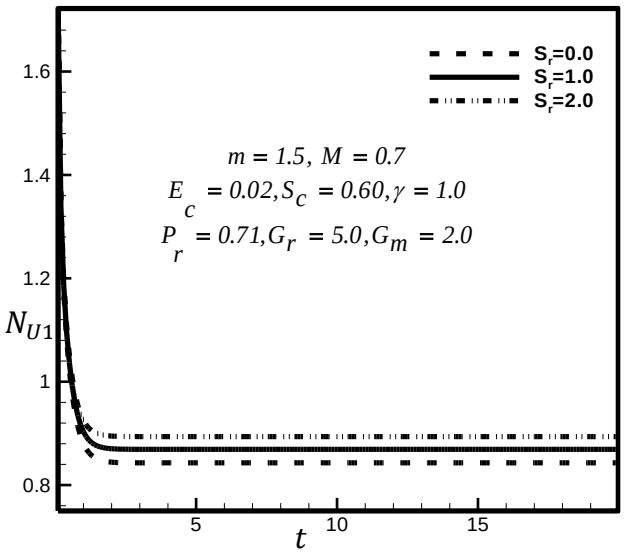

Fig. 19. Nusselt number at moving plate for different values of Soret number at $t = 5.0$

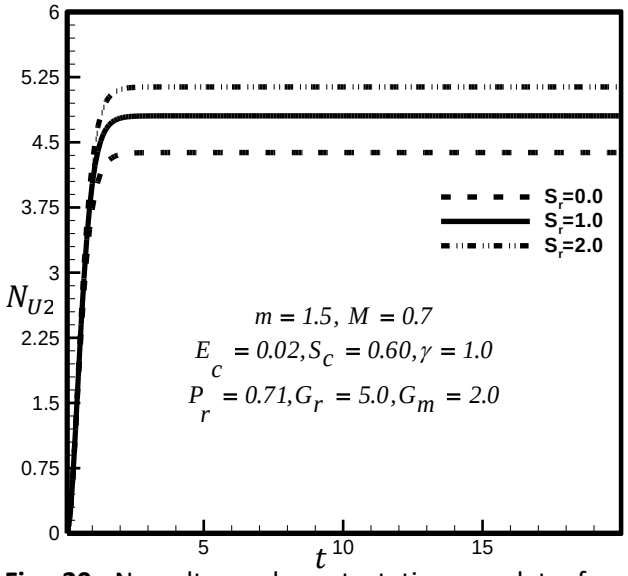

Fig. 20. Nusselt number at stationary plate for different values of Soret number at $t = 5.0$

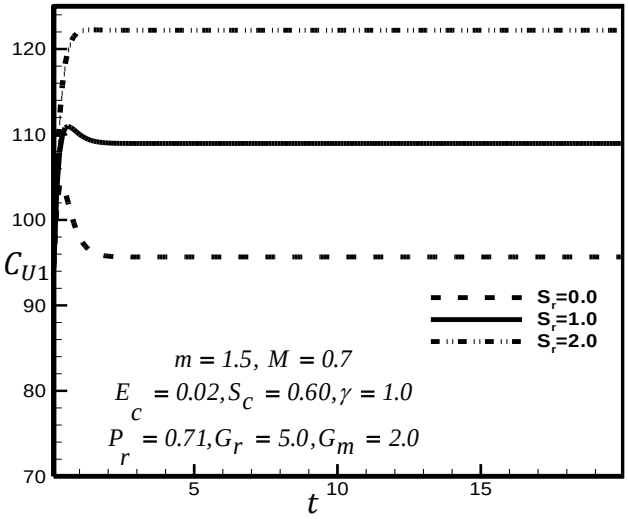

Fig. 21. Sherwood number at moving plate for different values of Soret number at $t = 5.0$

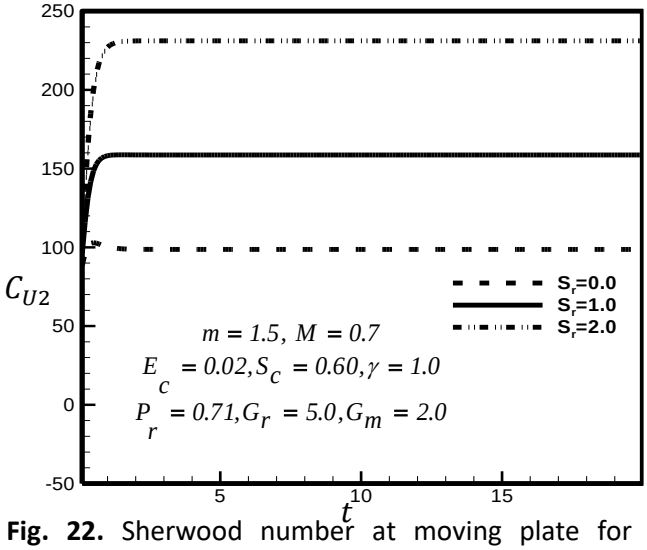

Fig. 22. Sherwood number at moving plate for different values of Soret number at $t = 5.0$

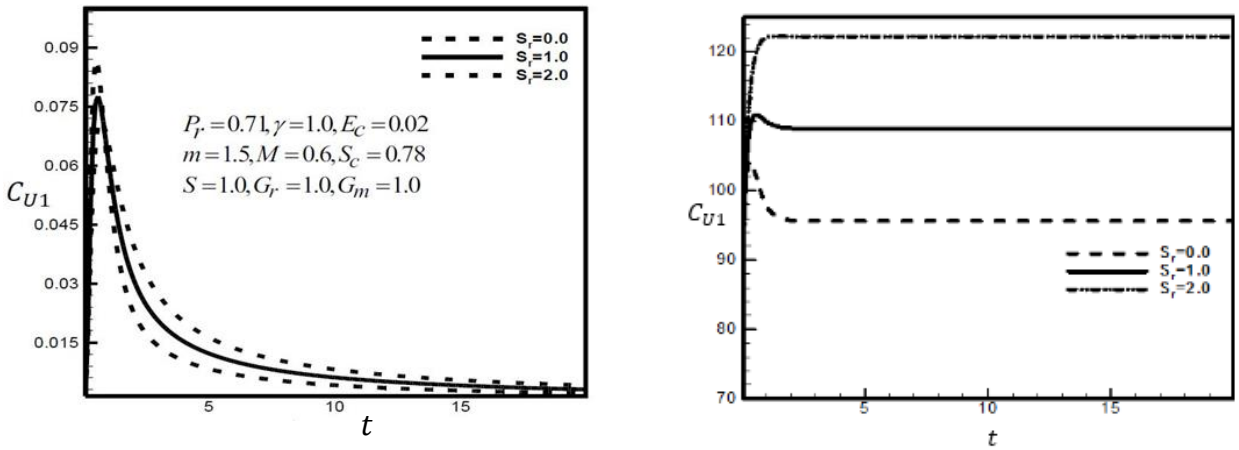

(a) (b)

Fig. 23. Comparison of Sherwood number for moving plate (a) Afikuzzaman and Alam work [14] (b) Present work

5. Conclusions

MHD Viscous Incompressible Casson Fluid Flow with Hall Current under the action of mass transfer by using explicit finite difference method (EFDM) has been taken into consideration. The physical properties are graphically discussed for different values of corresponding parameters. It is identified that, Hall term affects the primary velocity component and gives rise to another velocity component known as secondary velocity. The time at which temperature distributions reaches its steady state increases with increasing the m. The primary velocity, secondary velocity, temperature distribution and concentration distributions increase with the increase of S_r while it decreases with the increase of M .The shear stress increases both upper and lower plate with the increase of S_r but decreases with the increase of M . The Nusselt number increases both upper and lower plate with the increase of S_r but decreases with the increase of M . The Sherwood number increases both upper and lower plate with the increase of S_r but decreases with the increase of M .

Acknowledgement

This work is financed and supported by National Science and Technology under Ministry of Science and Technology, Government of the People's Republic of Bangladesh.

References

[1] Jha, Basant K., and Clement A. Apere. "Magnetohydrodynamic free convective Couette flow with suction and injection." *Journal of Heat Transfer* 133, no. 9 (2011): 1-12.
[2] Soundalgekar, V. M., N. V. Vighnesam, and H. S. Takhar. "Hall and ion-slip effects in MHD Couette flow with heat transfer." *IEEE Transactions on Plasma Science* 7, no. 3 (1979): 178-182.
[3] Das, Bigyani, and R. L. Batra. "Secondary flow of a Casson fluid in a slightly curved tube." *International journal of non-linear mechanics* 28, no. 5 (1993): 567-577.
[4] Huang, Kuo-Hsiung, and J. W. Yeh. "A study on the multicomponent alloy systems containing equal-mole elements." *Hsinchu: National Tsing Hua University* (1996).
[5] Walawender, Walter P., Te Yu Chen, and David F. Cala. "An approximate Casson fluid model for tube flow of blood." *Biorheology* 12, no. 2 (1975): 111-119.
[6] Batra, R. L., and Bigyani Jena. "Flow of a Casson fluid in a slightly curved tube." *International journal of engineering science* 29, no. 10 (1991): 1245-1258.
[7] Abdalla, I. A., Hazem Ali Attia, and Mohamed Eissa Sayed-Ahmed. "Adomian's Polynomial Solution of Unsteady Non-Newtonian MHD Flow." *Applied Mathematics & Information Sciences* 1, no. 3 (2007): 227-245.
[8] Beng, Soo Weng, and Wan Mohd Arif Aziz Japar. "Numerical analysis of heat and fluid flow in microchannel heat sink with triangular cavities." *Journal of Advanced Research In Fluid Mechanics And Thermal Sciences* 34, no. 1 (2017): 1-8.
[9] Pramanik, S. "Casson fluid flow and heat transfer past an exponentially porous stretching surface in presence of thermal radiation." *Ain Shams Engineering Journal* 5, no. 1 (2014): 205-212.
[10] Animasaun, I. L., E. A. Adebile, and A. I. Fagbade. "Casson fluid flow with variable thermo-physical property along exponentially stretching sheet with suction and exponentially decaying internal heat generation using the homotopy analysis method." *Journal of the Nigerian Mathematical Society* 35, no. 1 (2016): 1-17.
[11] Attia, Hazem Ali, and Mohamed Eissa Sayed-Ahmed. "Hydromagnetic Impulsively Lid-driven Flow and Heat Transfer of A Casson Fluid." *Tamkang Journal of Science and Engineering* 9, no. 3 (2006): 195-204.
[12] Sayed-Ahmed, M. E., Hazem A. Attia, and Karem M. Ewis. "Time dependent pressure gradient effect on unsteady mhd Couette flow and heat transfer of a Casson fluid." *Engineering* 3, no. 01 (2011): 38-49.
[13] Afikuzzaman, Md, M. Ferdows, and Md Mahmud Alam. "Unsteady MHD casson fluid flow through a parallel plate with hall current." *Procedia Engineering* 105 (2015): 287-293.
[14] Afikuzzaman, Md, and Md Mahmud Alam. "MHD casson fluid flow through a parallel plate." *Science & Technology Asia* 21, no. 1 (2016): 59-70.
[15] Wahiduzzaman, M., Md Tajul Islam, Parvin Sultana, and M. Afikuzzaman. "MHD couette flow of a Casson fluid between parallel porous plates." *Progress in Nonlinear Dynamics and Chaos* 2, no. 2 (2014): 51-60.

[16] Kataria, Hari R., and Harshad R. Patel. "Soret and heat generation effects on MHD Casson fluid flow past an oscillating vertical plate embedded through porous medium." *Alexandria Engineering Journal* 55, no. 3 (2016): 2125-2137.
[17] Oyelakin, Ibukun Sarah, Sabyasachi Mondal, and Precious Sibanda. "Unsteady Casson nanofluid flow over a stretching sheet with thermal radiation, convective and slip boundary conditions." *Alexandria engineering journal* 55, no. 2 (2016): 1025-1035.
[18] Sidra Aman, S. M., Z. Zokri, M. Z. Ismail, and Khan I. Salleh. "Effect of MHD and porosity on exact solutions and flow of a hybrid casson-nanofluid." *Journal of Advanced Research Fluid Mechanics and Thermal Science* 44, no. 1 (2018): 131-139.
[19] Mackolil, Joby, and Basavarajappa Mahanthesh. "Exact and statistical computations of radiated flow of nano and Casson fluids under heat and mass flux conditions." *Journal of Computational Design and Engineering* (2019).
[20] Liu, Chunyan, Liancun Zheng, Ping Lin, Mingyang Pan, and Fawang Liu. "Anomalous diffusion in rotating Casson fluid through a porous medium." *Physica A: Statistical Mechanics and its Applications* 528 (2019): 1-12.